Osteoarthritis and Cartilage Open 7 (2025) 100589

Contents lists available at ScienceDirect

Osteoarthritis and Cartilage Open

journal homepage: www.elsevier.com/journals/osteoarthritis-and-cartilage-open/2665-9131

Early age-related changes to articular cartilage $T_{1\rho}$ in hips with Legg–Calvé–Perthes disease deformity

Luke G. Johnson [a,b,c,*], Carly E. Jones [a,b], Daniel G. Rosenbaum [d], Benjamin Joseph [e], Emily K. Schaeffer [c], Kishore Mulpuri [c,f], David R. Wilson [a,b,c,f]

[a] School of Biomedical Engineering, University of British Columbia, Vancouver, BC, Canada
[b] Centre for Aging SMART, Vancouver Coastal Health, Vancouver, BC, Canada
[c] British Columbia Children's Hospital Research Institute, Vancouver, BC, Canada
[d] Department of Radiology, University of British Columbia, Vancouver, BC, Canada
[e] Department of Paediatric Orthopaedics, Kasturba Medical College, Manipal, Karnataka, India
[f] Department of Orthopaedics, University of British Columbia, Vancouver, BC, Canada

ARTICLE INFO

Handling Editor: Professor H Madry

Keywords:
Legg–Calvé–Perthes disease
Hip
Quantitative MRI
$T_{1\rho}$ imaging
Osteoarthritis

ABSTRACT

Objective: To determine whether the relationship between cartilage $T_{1\rho}$ relaxation time and age during adolescence and young adulthood is different in hips with Legg–Calvé–Perthes disease (LCPD) deformity compared to hips without LCPD deformity.

Design: We recruited 17 participants with LCPD deformity and 15 control participants aged 10–25 years in this frequency-matched cohort study. Quantitative magnetic resonance images were obtained for both hips in LCPD participants and one hip from each control using a $T_{1\rho}$ MAPSS sequence. The average $T_{1\rho}$ relaxation time in the weight-bearing articular cartilage was calculated, and we tested the interacting effects of age and participant group (LCPD vs non-LCPD) or subgroup (control, contralateral LCPD, spherical LCPD, and aspherical LCPD) on $T_{1\rho}$ using mixed effects models.

Results: The main effect of age on $T_{1\rho}$ relaxation time in hips without LCPD deformity was −0.63 ms/year (95 % confidence interval [−0.94, −0.32]). The age-adjusted main effect of LCPD deformity was +2.93 ms [0.65, 3.42] and the interaction effect of age and LCPD deformity was +0.46 ms/year [0.16, 0.76]. Moderate differences were observed between control and contralateral LCPD subgroups, and between spherical LCPD and aspherical LCPD subgroups.

Conclusions: Age-related changes in $T_{1\rho}$ relaxation time differ between hips with and without LCPD deformity, suggesting that cartilage degradation in LCPD is progressive and begins early in the healed stage of LCPD. By young adulthood, the difference in $T_{1\rho}$ between LCPD and non-LCPD hips is clinically important when considering osteoarthritis progression and outcomes.

1. Introduction

Legg–Calvé–Perthes disease (LCPD) is a self-resolving pediatric hip disorder caused by a disruption of blood supply to the femoral head. During the natural history of LCPD, the femoral head undergoes stages of necrosis, collapse, and reossification before the joint is considered "healed", 2–3 years later [1]. Although some hips return to a normal shape, patients often heal with a permanent residual deformity of the hip. Some residual LCPD deformities are associated with chondrolabral defects visible on magnetic resonance images (MRI), such as cartilage delamination or labral tears [2]. Greater deformity severity, measured with the Stulberg classification [3], is associated with early-onset hip osteoarthritis (OA) at follow-up [4,5]. One multi-center study with an average follow-up of 20.4 years post-onset (age 22–35 years) found radiographic OA (Tönnis grade II or higher) in 41 % of patients, and that 5 % had already had a total hip replacement [6].

Treatment of LCPD during the active stages of the disease focuses on maintaining hip congruence and containment [7], and may include non-weightbearing, range-of-motion physiotherapy, or varus osteotomy [8]. Once patients reach the "healed" stage of LCPD, options for

* Corresponding author. Centre for Aging SMART, 7/F, 2635 Laurel Street, Vancouver, BC, V5Z 1M9, Canada.
E-mail addresses: luke.johnson@ubc.ca (L.G. Johnson), carly.jones@ubc.ca (C.E. Jones), daniel.rosenbaum@cw.bc.ca (D.G. Rosenbaum), bjosephortho@yahoo.co.in (B. Joseph), emily.schaeffer@cw.bc.ca (E.K. Schaeffer), kmulpuri@cw.bc.ca (K. Mulpuri), david.wilson@ubc.ca (D.R. Wilson).

https://doi.org/10.1016/j.ocarto.2025.100589
Received 18 February 2025; Accepted 19 February 2025

long-term management are limited, with systematic guidelines for surgical intervention available only in the most severe symptomatic cases [9,10]. Non-surgical interventions such as physiotherapy and steroid injections are also employed [11], however the effectiveness and optimal timing of these strategies at preventing cartilage degradation during the healed stage of LCPD is unclear. Currently, patients with LCPD deformity receive treatment in response to symptoms [12,13]. It is unknown whether preventative management from the point of healing could delay the onset of OA and improve overall quality of life for LCPD patients.

Improving management of residual LCPD deformity requires a better understanding of the extent and timing of cartilage degradation in LCPD. Quantitative MRI techniques such as delayed gadolinium-enhanced MRI of cartilage (dGEMRIC) [14,15] and $T_{1\rho}$ [16–19] reflect cartilage degradation before lesions are visible in conventional MRI. In dGEMRIC sequences, T_1 contrast is proportional to proteoglycan (PG) content due to the diffusion of contrast agent into PG-depleted regions [20]. However, gadolinium contrast agents require IV placement and are associated with rare but potentially severe adverse reactions [20], limiting the use of dGEMRIC in children and adolescents. Alternatively, $T_{1\rho}$ sequences are sensitive to the concentration and quality of macromolecules in cartilage, including PGs and collagen, and can be used as a surrogate measure for cartilage health more broadly without contrast agents [21]. Reduced T_{1Gd} on dGEMRIC and elevated $T_{1\rho}$ (both indicating cartilage degradation) have been observed in hips with LCPD deformity compared to unaffected contralateral hips and normal control hips [4,22]. However, it is unclear whether these biochemical changes begin after healing or earlier in the disease evolution [23].

A primary limitation to interpreting the current quantitative MRI evidence in LCPD is the lack of a clear understanding of how $T_{1\rho}$ changes with age in hips without LCPD deformity. Past work in quantitative MRI [24] and animal studies [25,26] has shown biochemical changes in articular cartilage during normal growth, but the combined impact of these changes on $T_{1\rho}$ relaxation time is unclear. Without confirmation of the presence and magnitude of $T_{1\rho}$ changes in normal adolescent hips and contralateral hips in LCPD patients, our ability to study $T_{1\rho}$ changes with age in LCPD is limited. It is also unclear whether there are differences between unaffected contralateral hips in LCPD patients and normal hips representative of the adolescent and young adult population, and whether changes in $T_{1\rho}$ with age are similar in hips with spherical (Stulberg I/II) [3] and aspherical (Stulberg III-V) LCPD deformity.

In this study, our objective is to characterize the trajectory of cartilage degradation in adolescents and young adults with and without residual deformity from LCPD using $T_{1\rho}$ imaging. Our primary research question is.

- Does the relationship between $T_{1\rho}$ relaxation time and age differ between hips with and without residual LCPD deformity?

We have two secondary research questions.

- Does the relationship between $T_{1\rho}$ relaxation time and age differ between normal control hips and contralateral hips in LCPD participants?
- Is the relationship between $T_{1\rho}$ relaxation time and age affected by radiographic deformity severity in LCPD hips?

2. Methods

2.1. Participant recruitment

This frequency-matched cohort study was approved by the University of British Columbia Children's and Women's Research Ethics Board (Vancouver, BC, Canada) and is in accordance with the Helsinki Declaration of 1975, as revised in 2000. Participants in this study, or their parents where applicable, gave their informed consent to take part. In cases where parental consent was obtained, assent was also obtained from the participant.

Participants with residual LCPD deformity were recruited from our pediatric hospital orthopedic clinic during routine follow-up appointments, or from a research database of patients who had been treated for LCPD at the clinic and had agreed to be contacted for research purposes. Recruitment took place between June 2021 and November 2023, and data were collected between July 2021 and February 2024. Participants were eligible if they had been diagnosed with LCPD, were in modified Waldenström stage IIIb or later, and were 10–30 years old. Participants were excluded if they could not have an MRI, e.g. due to claustrophobia or metal hardware in the hip.

The control group was recruited to match the age and sex distribution of the LCPD group. Control participants were recruited between March 2023 and March 2024 through a public call for volunteers, and data collection took place between August 2023 and April 2024. Control participants were eligible if they had not previously been diagnosed with a hip disorder.

2.2. Magnetic resonance imaging and analysis

Each participant attended one MRI scanning session to measure the primary outcome variable ($T_{1\rho}$ relaxation time). We scanned both hips in LCPD participants and one randomly selected hip in control participants using a 3T GE Discovery MR750 scanner (GE Healthcare, Chicago, IL, USA). The $T_{1\rho}$ mapping sequence was based on the spin-locking Magnetization-prepared Angle-modulated Partitioned *k*-space Spoiled gradient echo Snapshots (MAPSS) research sequence [17,27] (Table 1). We modified and tested the sequence for use in children with five protocol development sessions (one with a phantom and four with volunteers). The primary goal, to shorten the image acquisition duration, was achieved by reducing the sequence recovery time (T_{rec}) from 1.2s to 0.8s, balancing a reduced signal-to-noise ratio with a smaller risk of motion artifacts.

Calculation of $T_{1\rho}$ relaxation time from MRI followed a previously validated methodology [22]. One rater (LJ) segmented the femoral and acetabular cartilage in the load-bearing region of each hip from the images with $T_{SL} = 1$ ms. To avoid partial-volume effects, all slices with the femoral head visible were identified, after which the rater only segmented the middle third in the anterior-posterior direction. The $T_{1\rho}$ relaxation time for each voxel within this volume was calculated using *MATLAB* (The Mathworks Inc., Natick, MA, USA). An exponential curve was fit to the voxel signal intensity at $T_{SL} = 1$, 15, 30, and 45 ms. To ensure only valid cartilage was included, voxels where $R^2 < 0.7$ or $T_{1\rho} > 90$ ms were discarded. Finally, the average $T_{1\rho}$ relaxation time was calculated from the remaining voxels (Fig. 1).

To test intra-rater repeatability, the same rater repeated the segmentation and recalculated average $T_{1\rho}$ for both hips in four LCPD participants, selected to represent a wide variety of LCPD deformity, one month after the initial assessment. To estimate inter-scan repeatability of the MAPSS sequence, one healthy adult volunteer was scanned four consecutive times in one imaging session during protocol development.

Table 1
Imaging parameters for $T_{1\rho}$ MAPSS sequences.

Parameter	MAPSS $T_{1\rho}$ (coronal view)
Field of view (mm)	220
Slice thickness/gap (mm)	4/0
Matrix size	384 × 256
Number of slices	22
Spin lock times (T_{SL}) (ms)	1, 15, 30, 45
Recovery time (T_{rec}) (ms)	800
Spin-lock frequency (Hz)	300
Scan duration (min:sec)	8:09

MAPSS, Magnetization-prepared Angle-modulated Partitioned *k*-space Spoiled gradient echo Snapshots.

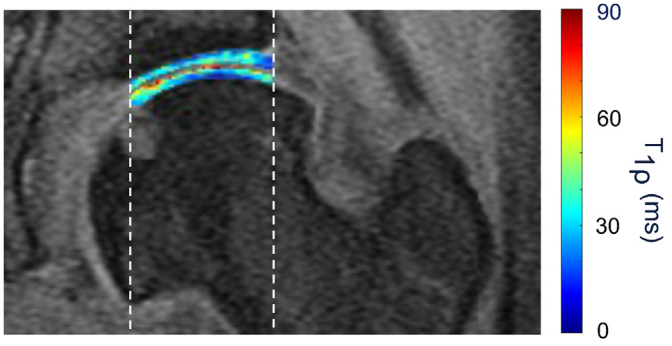

Fig. 1. $T_{1\rho}$ colormap of a hip with LCPD deformity (Stulberg grade IV). The weight-bearing articular cartilage, extending from the acetabular fossa to the acetabular rim, is indicated by vertical dashed lines. Acetabular and femoral cartilage are colorized by $T_{1\rho}$ relaxation time, with higher values suggesting worse cartilage health. LCPD, Legg–Calvé–Perthes disease.

2.3. Radiographic assessment

To answer our secondary research questions, the radiographic deformity severity was assessed for hips affected with LCPD. We obtained the most recent anteroposterior and frog-lateral pelvis radiographs from LCPD participants' clinical records. An expert rater (BJ) assessed the Stulberg classification [3] for every affected hip. Affected hips were grouped into two categories: spherical (Stulberg I/II) and aspherical (Stulberg III/IV/V). A second rater also independently assessed the Stulberg classification for all LCPD hips to determine inter-rater repeatability.

2.4. Statistical analysis

To answer our primary research question, we tested the hypothesis that the relationship between $T_{1\rho}$ relaxation time and age was different between hips with and without LCPD deformity using a mixed effects model (the *primary* model). The outcome variable was average $T_{1\rho}$ relaxation time across the whole load-bearing cartilage region, the interacting fixed effects were condition (non-LCPD and LCPD hips) and age, and patient was the random effect. Contralateral hips without LCPD deformity in patients who had had LCPD were included in the non-LCPD group.

To answer our secondary research questions, we split the participants' hips into four subgroups: normal control hips, unaffected contralateral hips in LCPD participants, hips with spherical (Stulberg I/II) LCPD deformity, and hips with aspherical (Stulberg III-V) LCPD deformity. We produced a second mixed effects model (the *subgroup* model) to determine whether contralateral hips in LCPD participants are different from control hips, and whether more severe aspherical LCPD deformity affects the trajectory of cartilage degradation.

Mixed models were chosen for our statistical analyses to account for missing data and the non-independence of paired hips in the dataset.

More severe aspherical radiographic deformity is associated with poorer patient-reported outcomes at long-term follow-up [6], which introduces a risk of response bias due to self-selection; participants who no longer have regular follow-up appointments may be more likely to respond to remote contact if they are experiencing symptoms. We expected that such a response bias could introduce an error into the interaction term (between LCPD deformity and age) of the primary mixed effects model, in which spherical and aspherical deformity groups were combined. We used a simulation approach to estimate the size of this error [28]. We created an *in silico* participant cohort with a uniform age distribution, and compared the distributions of $T_{1\rho}$ datasets generated from our primary mixed effects model, and from an alternative model with LCPD hips split into spherical and aspherical deformity groups. Complete details of our simulation methodology and results are included in Appendix A.

3. Results

We recruited 17 participants with residual LCPD deformity, from a total of 76 patients in the eligible age range that were contacted from the research database or were seen in the clinic during the recruitment period (Table 2). Participants with LCPD deformity were 11–24 years old, and four had had bilateral LCPD. One unilateral patient's affected hip was in modified Waldenström stage IIIb, with the remainder in stage IV. One hip in a patient with bilateral LCPD was excluded due to a metal screw in the joint.

Five LCPD hips had Stulberg grade I deformity, 5 grade II, 4 grade III, 5 grade IV, and 1 grade V. The inter-rater repeatability for the assessment of Stulberg grade was good (ICC = 0.76, 95 % CI [0.49, 0.90]). We recruited 15 control participants aged 10–25 years. The participant demographics and numbers of hips in each subgroup are summarized in Table 3.

Intra-rater repeatability for the calculation of average $T_{1\rho}$ relaxation time in the articular cartilage was excellent (ICC = 0.93, 95 % CI [0.69, 0.99]; RMSE = 0.99 ms). The coefficient of variation (CV) for inter-scan repeatability was 2.1 %. On average, 4.7 % of voxels were excluded from the $T_{1\rho}$ relaxation time calculation (range 0.0–19.1 %). In hips without and with LCPD deformity, the average exclusion rate was 3.5 % (0.0–19.1 %) and 6.6 % (0.4–17.4 %) respectively.

In the primary mixed effects model (Table 4 and Fig. 2), the age-adjusted main effect of LCPD deformity on $T_{1\rho}$ relaxation time, corresponding to the difference between non-LCPD and LCPD hips at the average participant age of 17.2 years, was +2.03 ms (95 % CI [0.65, 3.42]). The main effect of age on $T_{1\rho}$ was −0.63 ms/year [−0.94, −0.32] and the interaction effect of age and LCPD deformity was +0.46 ms/year [0.16, 0.76]. The model's prediction of $T_{1\rho}$ relaxation time in hips with LCPD deformity was 5.64 ms higher [2.83, 8.46] than in hips without LCPD deformity at age 25 years.

In the subgroup mixed effects model (Table 5 and Fig. 3), there was a significant overall interaction effect between participant subgroup and age (p = 0.016). The main effect of age on $T_{1\rho}$ relaxation time in control hips was −0.82 ms/year (95 % CI [−1.24, −0.4]) and $T_{1\rho}$ was also predicted to decrease with age in contralateral hips in LCPD patients (−0.47 ms/year [−0.88, −0.06]). The interaction effect of age and subgroup was significant in hips with aspherical LCPD deformity (+0.89 ms/year [0.23, 1.55]). The $T_{1\rho}$ prediction at age 10 was higher for control hips than all LCPD subgroups (including contralateral), and higher at age 25 in hips with LCPD deformity compared to control and

Table 2
Numbers of patients with LCPD deformity on the research contact database or who had clinical appointments at BC Children's Hospital during the recruitment period. Patients were not required to provide a reason for non-participation in this study.

Research contact database	
Total patients in eligible age range	**52**
Participants	14
Non-participants	38
Non-response to initial contact	*22*
No reason provided	*11*
Time constraints	*3*
Ineligible for MRI	*1*
Bad previous experience of MRI	*1*
Clinical follow-up visits[a]	
Total patients in eligible age range	**24**
Participants	3
Non-participants	21
No reason provided	*15*
Missed in clinic	*4*
Not interested in research	*1*
Language barrier	*1*

MRI, Magnetic Resonance Imaging.
[a] Excluding patients already on the research contact database.

Table 3
Participant demographics.

Participant group	# of participants (M/F)	Age (years) [mean (SD)]	# of hips
Control	15 (13 M 2F)	17.4 (4.7)	15
LCPD	17 (15 M 2F)	17.0 (4.7)	20
LCPD subgroups			
Spherical LCPD (Stulberg I/II)	*9[a] (9 M 0F)*	*15.1 (4.3)*	*10*
Aspherical LCPD (Stulberg III-V)	*9[a] (7 M 2F)*	*18.8 (4.2)*	*10*
Contralateral unaffected	*13 (11 M 2F)*	*16.8 (4.8)*	*13*

LCPD, Legg–Calvé–Perthes disease; SD, standard deviation.
[a] One participant with bilateral LCPD had one hip in each of the spherical and aspherical deformity groups and is included in both rows.

Table 4
Linear mixed effects predictions for age-adjusted $T_{1\rho}$ relaxation time, and $T_{1\rho}$ relaxation time trajectory (association with age) in hips with and without LCPD deformity. For hips with LCPD deformity, the differences in the mixed effects predictions from hips without LCPD deformity are also presented.

Mixed effects prediction	Hip groups		*Difference (95 % CI)*
	Non-LCPD ($n = 28$) (95 % CI)	LCPD ($n = 20$) (95 % CI)	
Age-adjusted $T_{1\rho}$ relaxation time (ms)	38.4 (36.9, 39.8)	40.4 (38.8, 42.0)	*2.03[a] (0.65, 3.42)* ***(p = 0.005)***
$T_{1\rho}$ relaxation time trajectory (ms/year)	−0.63[b] (−0.94, −0.32) **(p = 0.0002)**	−0.17 (−0.52, 0.19) (p = 0.35)	*0.46[c] (0.16, 0.76)* ***(p = 0.0036)***

CI, confidence interval; LCPD, Legg–Calvé–Perthes disease.
[a] Main effect of LCPD deformity.
[b] Main effect of age.
[c] Interaction effect of LCPD deformity and age.

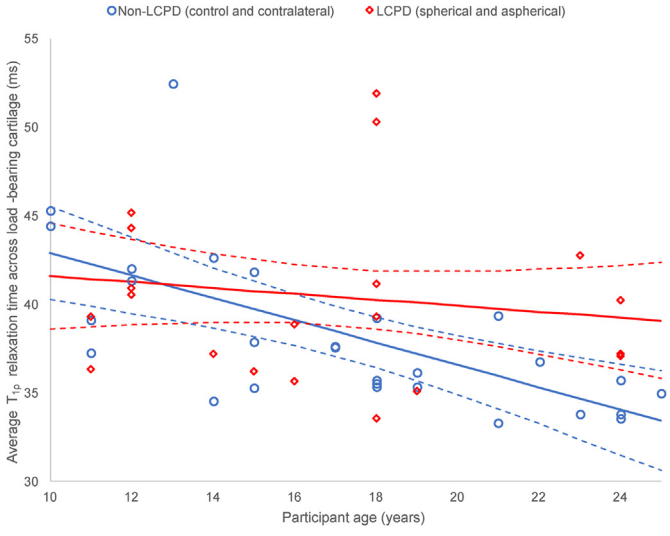

Fig. 2. $T_{1\rho}$ relaxation time in the weight-bearing articular cartilage plotted against chronologic age for all hips. The mixed effects prediction of the association between $T_{1\rho}$ and age is shown for hips without LCPD deformity (blue) and hips with LCPD deformity (red). Dashed lines indicate 95 % confidence intervals. LCPD, Legg–Calvé–Perthes disease.

contralateral subgroups (Fig. 3). However, differences at both age levels were only significant between the control and aspherical LCPD subgroups; −6.66 ms [−12.57, −0.74] at age 10, and +6.73 ms [1.23, 12.23] at age 25.

Diagnostic plots for both mixed effects models are included in Appendix A.

The average age of the aspherical LCPD deformity group was 3.7 years older than the spherical deformity group, likely due to self-selection of patients with severe radiographic deformity who had developed symptoms. When all hips with LCPD deformity were combined for our primary mixed effects model, this response bias was estimated to have increased the age-adjusted main effect of LCPD deformity on $T_{1\rho}$ relaxation time by +0.20 ms, and to have decreased the observed interaction effect of LCPD deformity and age by −0.015 ms/year.

4. Discussion

In this study, we found that $T_{1\rho}$ relaxation time in hips with residual LCPD deformity does not follow the same decreasing relationship with age seen in hips without LCPD deformity. Both groups are projected to have similar $T_{1\rho}$ at the age of 10 years but diverge through adolescence and young adulthood, ending up with substantially different $T_{1\rho}$ at the age of 25. Our subgroup analysis suggests that there may be differences between normal control hips and contralateral hips in younger patients, and that changes to $T_{1\rho}$ may be clinically relevant in hips with "mild" spherical LCPD deformity as well as aspherical deformity at age 25.

Our $T_{1\rho}$ findings in healthy hips are consistent with previous quantitative MRI studies. Our mixed effects prediction of $T_{1\rho}$ relaxation time in young adult hips without LCPD deformity (33.4 ms at age 25) is similar to previous measurement of $T_{1\rho}$ in healthy adult hips [29] (acetabular $T_{1\rho} = 32.7$ ms, femoral $T_{1\rho} = 35.2$ ms, age 43.6 ± 12.8 years), using the same MAPSS sequence as the present work. The observed relationship between $T_{1\rho}$ and age in hips without LCPD deformity is also consistent with other work on how cartilage changes during childhood and adolescence. T_2 relaxation time in cartilage, often used as a surrogate for collagen integrity, has been shown to decrease with chronologic age during childhood and adolescence [24]. Animal studies have demonstrated that PG content increases during development [25,26]. Our observations of the relationship between $T_{1\rho}$ and chronologic age in hips without LCPD deformity reflect normal biochemical changes in cartilage during development and establish a baseline against which LCPD-affected hips can be compared.

The relationship between $T_{1\rho}$ and age differs significantly between hips with LCPD deformity and healthy hips, suggesting that pre-OA biochemical changes in weight-bearing cartilage in LCPD are primarily progressive and begin after healing. Vijayan et al. [23] proposed two hypotheses for the timing of such changes: either beginning at the onset of LCPD, or starting at a later stage, likely in response to the mechanical environment of residual deformity. The results from our primary mixed effects model provide evidence to suggest the latter hypothesis has a larger contribution in the long run, and predict that cartilage degradation in LCPD is clinically important before the age of 25. At this age, the average LCPD hip is expected to have a $T_{1\rho}$ relaxation time 5.64 ms higher (17 %) than a typical hip without LCPD deformity. By comparison, the difference in $T_{1\rho}$ relaxation time between OA non-progressors (36.0 ms) and progressors (38.1 ms) is only 6 %, measured with the same MAPSS sequence in adults with a mean age of 46.5 ± 13.2 years [17], although these results may not be representative of the results observed in the present study's younger cohort. Grammatopoulos et al. [30] proposed a 17.6 % threshold for clinical significance, based on an inter-scan CV of 9 % from repeated 1.5T scans within a period of two weeks [31]. We estimated an improved inter-scan CV of 2.1 % for the MAPSS sequence at 3T, consistent with intra-site CVs of 1.6–3.93 % observed in the knee at 3T [32].

Our subgroup analysis, although statistically weaker, has indicated interesting trends that warrant further investigation. The prediction for $T_{1\rho}$ was substantially higher in control hips compared to all LCPD subgroups, including contralateral, at age 10 (Fig. 3), which suggests that cartilage biochemistry in younger patients may be influenced by possible systemic responses to LCPD, or earlier etiological factors such as alteration of the insulin-like growth factor-1 pathway [33,34]. As such, the hypothesis of early alteration to cartilage biochemistry [23] may still

Table 5
Linear mixed effects predictions for age-adjusted $T_{1\rho}$ relaxation time, and $T_{1\rho}$ relaxation time trajectory (association with age) in control hips, contralateral hips in LCPD patients, hips with spherical (Stulberg I/II) LCPD deformity, and hips with aspherical (Stulberg III-V) LCPD deformity. For all hips (affected and contralateral) in LCPD patients, the differences in the mixed effects predictions from control hips are also presented.

Mixed effects prediction	Hip subgroups				*Difference from control hips*		
	Control ($n = 15$) (95 % CI)	Contralateral ($n = 13$) (95 % CI)	Spherical LCPD ($n = 10$) (95%CI)	Aspherical LCPD ($n = 10$) (95%CI)	*Contralateral (95 % CI)*	*Spherical LCPD (95%CI)*	*Aspherical LCPD (95%CI)*
Age-adjusted $T_{1\rho}$ relaxation time (ms)	39.6 (37.7, 41.5)	37.2 (35.3, 39.0)	39.4 (37.1, 41.6)	39.4 (37.2, 41.6)	*−2.48*[a] *(−5.14, 0.19) (p = 0.068)*	*−0.24*[a] *(−3.18, 2.70) (p = 0.87)*	*−0.24*[a] *(−3.12, 2.64) (p = 0.87)*
$T_{1\rho}$ relaxation time trajectory (ms/year)	−0.82[b] (−1.24, −0.40) **(p = 0.0003)**	−0.47 (−0.88, −0.06) **(p = 0.025)**	−0.17 (−0.67, 0.32) (p = 0.48)	0.07 (−0.44, 0.58) (p = 0.78)	*0.35*[c] *(−0.23, 0.93) (p = 0.23)*	*0.65*[c] *(−0.00, 1.30) (p = 0.050)*	*0.89*[c] *(0.23, 1.55)* ***(p = 0.0092)***

CI, confidence interval; LCPD, Legg–Calvé–Perthes disease.
[a] Main effect of hip subgroup.
[b] Main effect of age.
[c] Interaction effect of hip subgroup and age.

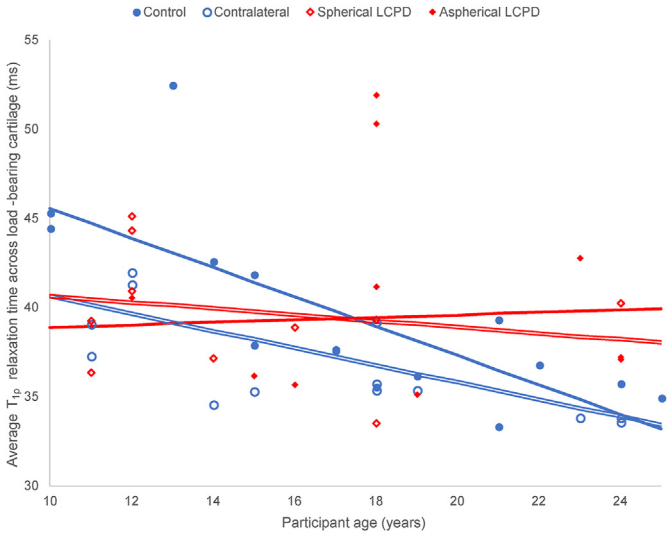

Fig. 3. $T_{1\rho}$ relaxation time in the weight-bearing articular cartilage plotted against chronologic age for all hips. The mixed effects prediction of the association between $T_{1\rho}$ and age is shown for control hips (blue, filled), contralateral hips in LCPD patients (blue, outline), hips with spherical LCPD deformity (red, outline) and hips with aspherical LCPD deformity (red, filled). LCPD, Legg–Calvé–Perthes disease.

contribute substantially in the years immediately after healing. By age 25, control and contralateral hips do not appear to differ (Fig. 3), suggesting that LCPD deformity is the dominant factor in young adults. The differences of the spherical and aspherical LCPD subgroups from the control subgroup are 4.82 ms and 6.73 ms (15 % and 20 %) respectively at age 25. Cartilage degradation is not only clinically important in hips with severe LCPD deformity but may also be substantial in "mild" spherical LCPD hips.

A key strength of our approach is that $T_{1\rho}$ imaging requires no contrast agents, avoiding the potential for rare but severe side-effects inherent in some other approaches. This allowed us to study a wide age range, with participants as young as 10 years, and to recruit control participants to characterize changes in $T_{1\rho}$ with age in normal adolescents and young adults. Mixed model diagnostic plots (Appendix A) showed good normality, linearity and homoscedasticity characteristics in both models. The assumption that changes in $T_{1\rho}$ over time are linear is therefore appropriate in this age range. Additionally, $T_{1\rho}$ MAPSS sequences have a lower specific absorption rate than the CubeQuant sequence used in previous work [22], which allowed us to improve the image quality.

One limitation of this study is that participants were not followed longitudinally, which would have been optimal for assessing the effect of age on $T_{1\rho}$. In addition, accurate records for time since healing or osteologic age were not available, both of which may provide a clearer understanding of the progression of cartilage degradation than chronologic age. Another limitation is that, due to the low prevalence of LCPD, the sample size is small (20 affected hips from 17 patients), but this is comparable with other MRI studies of LCPD [35–37]. The cohort was also self-selecting, resulting in a response bias towards more severe radiographic outcomes in older participants; participants who no longer had regular follow-up appointments may have been more likely to respond to contact if they had developed symptoms. Using a simulation approach, we estimated the effect of this bias to be small compared to the overall effect of LCPD deformity, contributing 9.4 % of the age-adjusted main effect and reducing the observed interaction effect by 3.3 %. Neither of these potential effects impact the conclusions of our statistical analysis. A further limitation is that we were unable to stratify by sex or gender in our statistical analysis, as we had only two female LCPD participants. The sex distribution of our LCPD group is consistent with the far higher prevalence of LCPD in boys than in girls [38]. It is difficult to synthesize our results with other studies, as $T_{1\rho}$ relaxation time measurements vary with MRI scanner manufacturer and sequence used [39]. For example, knee $T_{1\rho}$ measured using a CubeQuant sequence is 5.1 ms higher on average than $T_{1\rho}$ measured using a MAPSS sequence in the same scanner and participants [40].

$T_{1\rho}$ follows a different trajectory with age in hips with residual LCPD deformity than in hips without LCPD deformity. Both groups are projected to have similar $T_{1\rho}$ at age 10 but $T_{1\rho}$ is substantially elevated, an indicator of poor cartilage health, in LCPD hips by age 25. This trajectory suggests that cartilage degradation in the long term is primarily a result of the mechanical environment in healed LCPD rather than biochemical changes earlier in the disease process. These results provide a better understanding of early cartilage changes in LCPD that may be a precursor to pain and early-onset OA, which is necessary to develop more systematic preventative management approaches to improve long-term quality of life for people with LCPD deformity.

Author contributions

LGJ and DRW take responsibility for the integrity of the work. Conception and design: LGJ, CEJ, DR, EKS, KM, DRW. Acquisition, analysis or interpretation of data: LGJ, BJ, DRW. Drafting the article: LGJ, DR, DRW. Critical review of the article: CEJ, BJ, EKS, KM. Final review of the version to be published: LGJ, CEJ, DR, BJ, EKS, KM, DRW. All authors agree to be accountable for all aspects of the work in ensuring that

questions related to the accuracy or integrity of any part of the work are appropriately investigated and resolved.

Role of the funding source

Funding for this work was provided by the Canadian Institutes of Health Research (Funding reference 165956). LGJ, EKS and KM are supported by the I'm a HIPpy Foundation and the Peterson Fund for Global Hip Health. LGJ is supported by Arthritis Society Canada (TGP22-0000000149). The funders had no role in the design and conduct of the study; collection, analysis, and interpretation of the data; preparation, review, or approval of the manuscript; and decision to submit the manuscript for publication.

Declaration of competing interest

The authors declare no conflict of interest relevant to this study.

Acknowledgements

We would like to thank Dr Vuong Nguyen for advising on this work's statistical analyses, and Dr Gourav Jandial for performing measurements of the Stulberg classification for repeatability.

Appendix A. Supplementary data

Supplementary data to this article can be found online at https://doi.org/10.1016/j.ocarto.2025.100589.

References

[1] B. Joseph, G. Varghese, K. Mulpuri, K.L.N. Rao, N. Sreekumaran Nair, Natural evolution of Perthes disease: a study of 610 children under 12 years of age at disease onset, J. Pediatr. Orthop. 23 (2003) 590–600, https://doi.org/10.1097/01241398-200309000-00005.

[2] D.A. Carvalho Maranho, M.H. Nogueira-Barbosa, A. Zamarioli, J.B. Volpon, MRI abnormalities of the acetabular labrum and articular cartilage are common in healed Legg-Calvé-perthes disease with residual deformities of the hip, J Bone Jt Surg 95 (2013) 256–265, https://doi.org/10.2106/JBJS.K.01039.

[3] S.D. Stulberg, D.R. Cooperman, R. Wallensten, The natural history of Legg-Calve-Perthes disease, J Bone Jt Surg 63A (1981) 1095–1108.

[4] C. Zilkens, A. Holstein, B. Bittersohl, M. Jäger, T. Haamberg, F. Miese, et al., Delayed gadolinium-enhanced magnetic resonance imaging of cartilage in the long-term follow-up after perthes disease, J. Pediatr. Orthop. 30 (2010) 147–153, https://doi.org/10.1097/BPO.0b013e3181cf13e6.

[5] Y.D. Hailer, E. Penno, Agreement of radiographic measurements and patient-reported outcome in 61 patients with Legg-Calvé-Perthes disease at mean follow-up of 28 years, J. Pediatr. Orthop. Part B 28 (2019) 100–106, https://doi.org/10.1097/BPB.0000000000000563.

[6] A.N. Larson, D.J. Sucato, J.A. Herring, S.E. Adolfsen, D.M. Kelly, J.E. Martus, et al., A prospective multicenter study of Legg-Calvé-perthes disease, J Bone Jt Surg 94 (2012) 584–592, https://doi.org/10.2106/JBJS.J.01073.

[7] H.K.W. Kim, Legg-calvé-Perthes disease, J. Am. Acad. Orthop. Surg. 18 (2010) 676–686, https://doi.org/10.5435/00124635-201011000-00005.

[8] J.A. Herring, H.T. Kim, R. Browne, Legg-Calve-Perthes disease. Part II: prospective multicenter study of the effect of treatment on outcome, J Bone Joint Surg Am 86 (2004) 2121–2134, https://doi.org/10.1007/978-1-4471-5451-8_146.

[9] M. Tannast, N. MacIntyre, S.D. Steppacher, H.S. Hosalkar, R. Ganz, K.A. Siebenrock, A systematic approach to analyse the sequelae of LCPD, HIP Int. 23 (2013) 61–70, https://doi.org/10.5301/hipint.5000071.

[10] C.E. Albers, S.D. Steppacher, R. Ganz, K.A. Siebenrock, M. Tannast, Joint-preserving surgery improves pain, range of motion, and abductor strength after Legg-Calvé-Perthes disease hip, Clin. Orthop. Relat. Res. 470 (2012) 2450–2461, https://doi.org/10.1007/s11999-012-2345-0.

[11] H.K.W. Kim, R. Almakias, M.B. Millis, B. Vakulenko-Lagun, How are adults who had Perthes' disease functioning? Bone Jt J 104B (2022) 1304–1312, https://doi.org/10.1302/0301-620X.104B12.BJJ-2022-0764.R1.

[12] D.A. Podeszwa, A. Delarocha, Clinical and radiographic analysis of perthes deformity in the adolescent and young adult, J. Pediatr. Orthop. 33 (2013) 56–61, https://doi.org/10.1097/BPO.0b013e31828111f6.

[13] T. Ng, R. Liu, V.A. Kulkarni, Legg-calvé-Perthes disease: diagnosis, decision making, and outcome, Curr. Sports Med. Rep. 23 (2024) 45–52, https://doi.org/10.1249/JSR.0000000000001139.

[14] C.J. Tiderius, L.E. Olsson, P. Leander, O. Ekberg, L. Dahlberg, Delayed gadolinium-enhanced MRI of cartilage (dGEMRIC) in early knee osteoarthritis, Magn. Reson. Med. 49 (2003) 488–492, https://doi.org/10.1002/mrm.10389.

[15] J.T. Samosky, D. Burstein, W.E. Grimson, R. Howe, S. Martin, M.L. Gray, Spatially-localized correlation of dGEMRIC-measured GAG distribution and mechanical stiffness in the human tibial plateau, J. Orthop. Res. 23 (2005) 93–101, https://doi.org/10.1016/j.orthres.2004.05.008.

[16] R.R. Regatte, S.V.S. Akella, J.H. Lonner, J.B. Kneeland, R. Reddy, T 1ρ relaxation mapping in human osteoarthritis (OA) cartilage: comparison of T 1ρ with T 2, J. Magn. Reson. Imag. 23 (2006) 547–553, https://doi.org/10.1002/jmri.20536.

[17] M.C. Gallo, C. Wyatt, V. Pedoia, D. Kumar, S. Lee, L. Nardo, et al., T1ρ and T2 relaxation times are associated with progression of hip osteoarthritis, Osteoarthr. Cartil. 24 (2016) 1399–1407, https://doi.org/10.1016/j.joca.2016.03.005.

[18] A. Borthakur, E. Mellon, S. Niyogi, W. Witschey, J.B. Kneeland, R. Reddy, Sodium and T 1ρ MRI for molecular and diagnostic imaging of articular cartilage, NMR Biomed. 19 (2006) 781–821, https://doi.org/10.1002/nbm.1102.

[19] F. Kogan, B.A. Hargreaves, G.E. Gold, Volumetric multislice gagCEST imaging of articular cartilage: optimization and comparison with T1rho, Magn. Reson. Med. 77 (2017) 1134–1141, https://doi.org/10.1002/mrm.26200.

[20] H.J. Braun, G.E. Gold, Advanced MRI of articular cartilage, Imag. Med. 3 (2011) 541–555, https://doi.org/10.2217/iim.11.43.

[21] V. Casula, J. Karjalainen, V. Mlynarik, T. Liimatainen, M. Hanni, E.H.G. Oei, et al., Does T1ρ measure proteoglycan concentration in cartilage? J. Magn. Reson. Imag. 59 (2024) 1874–1875, https://doi.org/10.1002/jmri.28981.

[22] C.E. Jones, K. Mulpuri, T. Teo, D.R. Wilson, A.G. D'Entremont, T1ρ and T2 MRI show hip cartilage damage in adolescents with healed Legg-Calvé-Perthes disease, J. Pediatr. Orthop. B 31 (2022) 344–349, https://doi.org/10.1097/BPB.0000000000000892.

[23] S. Vijayan, O. Mehta, G. Jacob, N.D. Siddesh, H. Shah, B. Joseph, The fate of the joint space in Legg-Calvé-Perthes' disease, Skelet. Radiol. 42 (2013) 341–345, https://doi.org/10.1007/s00256-012-1474-6.

[24] H.K. Kim, S. Shiraj, C.G. Anton, P.S. Horn, B.J. Dardzinski, Age and sex dependency of cartilage T2 relaxation time mapping in MRI of children and adolescents, Am. J. Roentgenol. 202 (2014) 626–632, https://doi.org/10.2214/AJR.13.11327.

[25] M.M. Hyttinen, J. Holopainen, P.R. van Weeren, E.C. Firth, H.J. Helminen, P.A.J. Brama, Changes in collagen fibril network organization and proteoglycan distribution in equine articular cartilage during maturation and growth, J. Anat. 215 (2009) 584–591, https://doi.org/10.1111/j.1469-7580.2009.01140.x.

[26] P. Julkunen, E.P. Halmesmäki, J. Iivarinen, L. Rieppo, T. Närhi, J. Marjanen, et al., Effects of growth and exercise on composition, structural maturation and appearance of osteoarthritis in articular cartilage of hamsters, J. Anat. 217 (2010) 262–274, https://doi.org/10.1111/j.1469-7580.2010.01270.x.

[27] X. Li, E.T. Han, R.F. Busse, S. Majumdar, In vivo T1ρ mapping in cartilage using 3D magnetization-prepared angle-modulated partitionedk-space spoiled gradient echo snapshots (3D MAPSS), Magn. Reson. Med. 59 (2008) 298–307, https://doi.org/10.1002/mrm.21414.

[28] H.R. Banack, E. Hayes-Larson, E.R. Mayeda, Monte Carlo simulation approaches for quantitative bias analysis: a tutorial, Epidemiol. Rev. 43 (2021) 106–117, https://doi.org/10.1093/epirev/mxab012.

[29] V. Pedoia, M.C. Gallo, R.B. Souza, S. Majumdar, Longitudinal study using voxel-based relaxometry: association between cartilage T1ρ and T2 and patient reported outcome changes in hip osteoarthritis, J. Magn. Reson. Imag. 45 (2017) 1523–1533, https://doi.org/10.1002/jmri.25458.

[30] G. Grammatopoulos, G. Melkus, K. Rakhra, P.E. Beaulé, Does cartilage degenerate in asymptomatic hips with cam morphology? Clin. Orthop. Relat. Res. 477 (2019) 962–971, https://doi.org/10.1097/CORR.0000000000000629.

[31] H. Anwander, K.S. Rakhra, G. Melkus, P.E. Beaulé, T1ρ hip cartilage mapping in assessing patients with cam morphology: how can we optimize the regions of interest? Clin. Orthop. Relat. Res. 475 (2017) 1066–1075, https://doi.org/10.1007/s11999-016-5011-0.

[32] J. Kim, K. Mamoto, R. Lartey, K. Xu, K. Nakamura, W. Shin, et al., Multi-vendor multi-site T1ρ and T2 quantification of knee cartilage, Osteoarthr. Cartil. 28 (2020) 1539–1550, https://doi.org/10.1016/j.joca.2020.07.005.

[33] M. Dixit, S.B. Poudel, S. Yakar, Effects of GH/IGF axis on bone and cartilage, Mol. Cell. Endocrinol. 519 (2021) 111052, https://doi.org/10.1016/j.mce.2020.111052.

[34] H.K.W. Kim, Legg-calve-Perthes disease: etiology, pathogenesis, and biology, J. Pediatr. Orthop. 31 (2011) S141–S146, https://doi.org/10.1097/BPO.0b013e318223b4bd.

[35] K.D. Standefer, M. Dempsey, C.H. Jo, H.K.W. Kim, 3D MRI quantification of femoral head deformity in Legg–Calvé–perthes disease, J. Orthop. Res. 35 (2017) 2051–2058, https://doi.org/10.1002/jor.23484.

[36] D. Pienkowski, J. Resig, V. Talwalkar, C. Tylkowski, Novel three-dimensional MRI technique for study of cartilaginous hip surfaces in Legg-Calvé-Perthes disease, J. Orthop. Res. 27 (2009) 981–988, https://doi.org/10.1002/jor.20909.

[37] A. Memiş, S. Varlı, F. Bilgili, A novel approach for computerized quantitative image analysis of proximal femur bone shape deformities based on the hip joint symmetry, Artif. Intell. Med. 115 (2021) 102057, https://doi.org/10.1016/j.artmed.2021.102057.

[38] D.C. Perry, The epidemiology and etiology of perthes' disease, in: K.-H. Koo, L.C. Jones (Eds.), Osteonecrosis, Springer Berlin Heidelberg, Berlin, Heidelberg, 2014, pp. 419–425, https://doi.org/10.1007/978-3-642-35767-1_58.

[39] B.L. Eck, M. Yang, J.J. Elias, C.S. Winalski, F. Altahawi, N. Subhas, et al., Quantitative MRI for evaluation of musculoskeletal disease: cartilage and muscle composition, joint inflammation, and biomechanics in osteoarthritis, Investig. Radiol. 58 (2023) 60–75, https://doi.org/10.1097/RLI.0000000000000909.

[40] M. Tanaka, V. Pedoia, D. Chandramohan, W. Chen, X. Li, Comparison of T1ρ quantification, SNR, and reproducibility in 3D magnetization-prepared angle-modulated partitioned k-space spoiled gradient echo snapshots (3D MAPSS). 3D Fast Spin Echo (CubeQuant) Techniques, 2017.